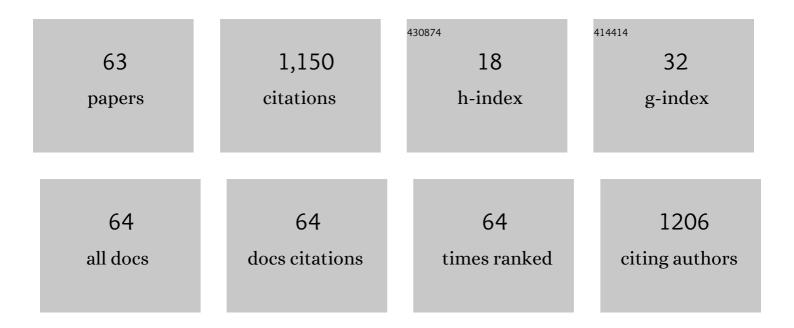
List of Publications by Year in descending order

Source: https://exaly.com/author-pdf/6534563/publications.pdf Version: 2024-02-01



ARTICLE IF CITATIONS Is Rhenium Diboride a Superhard Material?. Advanced Materials, 2008, 20, 4780-4783. 21.0 A comparative study of ZnAl2O4 nanoparticles synthesized from different aluminum salts for use as 3.3 124 fluorescence materials. Scientific Reports, 2015, 5, 12849. Insight into the optical, color, photoluminescence properties, and photocatalytic activity of the N–O and C–O functional groups decorating spinel type magnesium aluminate. CrystEngComm, 2019, 21, 2.6 263-277. Phase transitions of LiAlO2 at high pressure and high temperature. Journal of Solid State Chemistry, 2.9 52 2008, 181, 1810-1815. Synthetic Route to Metal Nitrides: High-Pressure Solid-State Metathesis Reaction. Inorganic 4.0 44 Chemistry, 2013, 52, 13356-13362. Pressure calibration for the cubic press by differential thermal analysis and the high-pressure fusion 1.2 40 curve of aluminum. High Pressure Research, 2009, 29, 806-814. A new route for the preparation of CoAl2O4 nanoblue pigments with high uniformity and its optical 2.4 properties. Journal of Sol-Gel Science and Technology, 2018, 86, 206-216. Synthesis of GaN Crystals Through Solid-State Metathesis Reaction Under High Pressure. Crystal 3.0 34 Growth and Design, 2009, 9, 1264-1266. Synthesis and Characterization of BaAl₂O₄ Catalyst and its Photocatalytic Activity Towards Degradation of Methylene Blue Dye. Zeitschrift Fur Physikalische Chemie, 2019, 233, 2.8 34 1161-1181. Li ion diffusion in LiAlO 2 investigated by Raman spectroscopy. Solid State Sciences, 2014, 37, 103-107. 3.2 29 Perovskiteâ€Type SrVO₃ as Highâ€Performance Anode Materials for Lithiumâ€Ion Batteries. 21.0 Advanced Materials, 2022, 34, e2107262. High-pressure and high-temperature sintering of nanostructured bulk NiAl materials. Journal of 2.6 25 Materials Research, 2009, 24, 2089-2096. Superstrong micro-grained polycrystalline diamond compact through work hardening under high 3.3 pressure. Applied Physics Letters, 2018, 112, . Recent advance in high-pressure solid-state metathesis reactions. Matter and Radiation at Extremes, 3.9 23 2018, 3, 95-103. GaN crystals prepared through solid-state metathesis reaction from NaGaO2 and BN under high pressure and high temperature. Journal of Alloys and Compounds, 2011, 509, L124-L127. Synthesis of Visible-Light-Driven SrAl2O4-Based Photocatalysts Using Surface Modification and Ion 0.6 22 Doping. Russian Journal of Physical Chemistry A, 2020, 94, 1234-1247.

17	Unusual Compression Behavior of Nanocrystalline CeO2. Scientific Reports, 2014, 4, 4441.	3.3	21
18	High pressure synthesis and properties studies on spherical bulk ϵ-Fe ₃ N. High Pressure	1.2	19

Research, 2014, 34, 317-326.

#

9

4

6

8

10

11

12

14

16

#	Article	IF	CITATIONS
19	Preparation of superhard cubic boron nitride sintered from commercially available submicron powders. Journal of Applied Physics, 2017, 121, .	2.5	18
20	Evidence for a New Extended Solid of Nitrogen*. Chinese Physics Letters, 2020, 37, 068101.	3.3	18
21	Rapid synthesis of thermoelectric SnSe thin films by MPCVD. RSC Advances, 2020, 10, 11990-11993.	3.6	17
22	Cation order–disorder phase transitions in LiGaO2: Observation of the pathways of ternary wurtzite under high pressure. Journal of Applied Physics, 2010, 108, .	2.5	16
23	Disorder-activated Raman spectra of cubic rocksalt-type Li(1â^' <i>x</i>)/2Ga(1â^' <i>x</i>)/2 <i>Mx</i> O (<i>M</i> = Mg, Zn) alloys. Journal of Applied Physics, 2012, 112, .	2.5	16
24	High-pressure Raman spectroscopy study of LiGaO2. Solid State Communications, 2013, 164, 6-10.	1.9	15
25	Abnormal physical behaviors of hafnium diboride under high pressure. Applied Physics Letters, 2019, 115, .	3.3	15
26	High-pressure x-ray diffraction study of YBO3/Eu3+, GdBO3, and EuBO3: Pressure-induced amorphization in GdBO3. Journal of Applied Physics, 2014, 115, .	2.5	14
27	Neutron diffraction study of the structural and magnetic properties of ε-Fe3N1.098 and ε-Fe2.322Co0.678N0.888. Journal of Alloys and Compounds, 2018, 752, 99-105.	5.5	13
28	High-pressure Raman spectroscopy of Re 3 N crystals. Solid State Communications, 2015, 201, 107-110.	1.9	12
29	Pressure induced solid-solid reconstructive phase transition in <mml:math xmlns:mml="http://www.w3.org/1998/Math/MathML"><mml:mrow><mml:mi>LiGa</mml:mi><mml:msub><mml:r mathvariant="normal">O<mml:mn>2</mml:mn></mml:r </mml:msub></mml:mrow> dominated by elastic strain. Physical Review B, 2018, 97, .</mml:math 	mi 3.2	10
30	Pressure-induced disordering of site occupation in iron–nickel nitrides. Matter and Radiation at Extremes, 2021, 6, .	3.9	10
31	Strengthening effects of interstitial nitrogen on rhenium. Journal of Applied Physics, 2018, 123, .	2.5	9
32	Raman study of pressure-induced dissociative transitions in nitrogen. Solid State Communications, 2019, 298, 113645.	1.9	9
33	Micro-stress dominant displacive reconstructive transition in lithium aluminate. Applied Physics Letters, 2016, 109, .	3.3	8
34	Enhancing the pressure limitation in large-volume Bridgman-anvil cell used for in situ neutron diffraction. High Pressure Research, 2019, 39, 655-665.	1.2	8
35	Melting temperature of diamond and cubic boron nitride at 15 gigapascals. Physical Review Research, 2019, 1, .	3.6	8
36	Pressure transmitting medium-dependent structure stability of nanoanatase TiO ₂ under high pressure. High Pressure Research, 2014, 34, 259-265.	1.2	7

#	Article	IF	CITATIONS
37	Reciprocating Compression of ZnO Probed by X-ray Diffraction: The Size Effect on Structural Properties under High Pressure. Inorganic Chemistry, 2018, 57, 5380-5388.	4.0	7
38	Neutron powder diffraction and high-pressure synchrotron x-ray diffraction study of tantalum nitrides. Chinese Physics B, 2018, 27, 026201.	1.4	6
39	Temperature-dependent c-axis lattice-spacing reduction and novel structural recrystallization in carbon nano-onions filled with Fe3C/ \hat{l} ±-Fe nanocrystals. Nano Express, 2020, 1, 020016.	2.4	6
40	High-pressure synthesis and in-situ high pressure x-ray diffraction study of cadmium tetraphosphide. Journal of Applied Physics, 2013, 113, 053507.	2.5	5
41	Effects of substitution, pressure, and temperature on the phonon mode in layered-rocksalt-type Li(1Ⱂx)/2Ga(1Ⱂx)/2ZnxO (x = 0.036–0.515) alloys. Journal of Applied Physics, 2015, 118, 185903.	2.5	5
42	Anomalous compression behavior of â^¼12 nm nanocrystalline TiO2. Journal of Applied Physics, 2017, 121, .	2.5	5
43	High-Pressure Synthesis of CeOCl Crystals and Investigation of Their Photoluminescence and Compressibility Properties. Crystal Growth and Design, 2018, 18, 1843-1847.	3.0	5
44	Highâ€pressure Raman spectroscopy of CeOCl: Observation of the isostructural phase transition. Journal of Raman Spectroscopy, 2019, 50, 1962-1968.	2.5	5
45	Ferromagnetic hysteresis and structural recrystallization in turbostratic graphite. Materials Research Express, 2019, 6, 105612.	1.6	5
46	Synthesis and characterization of spherical-like bulk Îμ-Fe3â^'Co N (xÂ=Â0.0, 0.25, 1.95). Materials Chemistry and Physics, 2017, 197, 94-99.	4.0	4
47	Pressure-Induced Structural Phase Transformation and Yield Strength of AlN. Journal of Physical Chemistry C, 2019, 123, 28437-28442.	3.1	4
48	Raman spectroscopy and phase stability of λ-N2. Solid State Communications, 2020, 310, 113843.	1.9	4
49	Raman spectroscopy and Xâ€ray diffraction of pressureâ€induced reversible structure change in K 2 OsO 2 (OH) 4. Journal of Raman Spectroscopy, 2020, 51, 1240-1247.	2.5	4
50	The effect of interstitial-site nitrogen on structural, elastic, and magnetic properties of face-center cubic Co. Journal of Applied Physics, 2021, 129, .	2.5	4
51	Observation of specific optical phonon modes dominating Li ion diffusion in γ-LiAlO2 ceramic. Ceramics International, 2021, 47, 17980-17985.	4.8	4
52	Evidence for a High-Pressure Isostructural Transition in Nitrogen. Chinese Physics Letters, 2022, 39, 026401.	3.3	4
53	Hysteresis effect in pressure-induced B4-B1 phase transition of ZnO. Materials Research Express, 2019, 6, 126502.	1.6	3
54	Ferromagnetic correlation in hydrogen doped highly oriented pyrolytic graphite. Diamond and Related Materials, 2020, 109, 108030	3.9	3

#	Article	IF	CITATIONS
55	Equation of state for generalized pressure. Physical Review B, 2022, 105, .	3.2	3
56	Enhanced hardness of CVD diamond after high pressure and high-temperature treatments. High Pressure Research, 2015, 35, 363-371.	1.2	2
57	Raman study of nonhydrostatic pressureâ€induced phase transitions in monoclinic Lâ€aspartic acid crystals. Journal of Raman Spectroscopy, 2019, 50, 1205-1216.	2.5	2
58	Coupling behavior between lattice dynamics and Li self-diffusion in layered α-LiAlO2 ceramic. Ceramics International, 2021, 47, 14587-14593.	4.8	2
59	The solubility behavior of NaCl in water at high pressure studied by neutron diffraction and Raman scattering. High Pressure Research, 2021, 41, 39-51.	1.2	1
60	The coupling of lattice-strain and phonon induced order-disorder phase transition in layered LiGaO2. Physics Letters, Section A: General, Atomic and Solid State Physics, 2021, 407, 127464.	2.1	1
61	High-pressure synthesis of TaN compacts with high hardness and thermal stability. Ceramics International, 2021, 47, 30039-30042.	4.8	1
62	High-pressure Raman study of osmium and rhenium up to 200 GPa and pressure dependent elastic shear modulus C 44. Chinese Physics B, 0, , .	1.4	0
63	Magnetic moment manipulation in hydrogen-peroxide-doped grafoil, pyrolytic graphite and Fe3C-filled multiwall carbon nanotubes. Nano Express, 2020, 1, 030027.	2.4	Ο